Theor Appl Climatol (2012) 110:395–408
DOI 10.1007/s00704-012-0636-8

ORIGINAL PAPER

Areal differences in diurnal variations in summer precipitation over Beijing metropolitan region

Jiali Wang · Renhe Zhang · Yingchun Wang

Received: 21 February 2011 / Accepted: 11 March 2012 / Published online: 30 March 2012

Abstract Using hourly rain-gauge measurements for the period 2004–2007, differences in diurnal variation in summer (June–August) precipitation are investigated in four distinct areas of Beijing: the urban area (UA), suburban area (SA), north mountainous area (NMA), and south mountainous area (SMA), which are distinguished empirically based on underlying surface conditions and verified with a statistical rotated empirical orthogonal function. The diurnal cycles and spatial patterns in seasonal mean precipitation amount, intensity, and frequency in the four areas are compared. Results show that the four areas have distinct diurnal variation patterns in precipitation amounts, with a single peak observed in UA and NMA in the late afternoon, which are 80 % and 121 % higher than their daily average, respectively, and two peaks in SA during the late afternoon and early morning with magnitudes exceeding the daily mean by 76 % and 29 %, respectively. There are also two peaks in SMA: a weaker nocturnal diurnal peak and an afternoon peak. The minimum amounts of rainfall observed in the forenoon in UA, SA, and SMA are 53 %, 47 %, and 57 % lower than the daily mean in each area, respectively, and that observed in the early morning in NMA is 50 % lower than the daily mean. The diurnal variations in precipitation intensities resemble those for precipitation amount in all four areas, but more intense precipitation is observed in SA (2.4 mm/h) than in UA (2.2 mm/h). The lowest frequency for the whole day is observed in UA, whereas the highest frequency occurs in the mountainous areas in the daytime, especially in the late afternoon in SMA. Diurnal variations in surface air temperature and divergence fields in the four areas are further investigated to interpret the physical mechanisms that underlie the spatial and temporal differences in summer diurnal precipitation, and the results indicate the possible dominance of the local circulation arising from mountain–valley wind and the differences in underlying surface heating between the urban, suburban, and mountainous areas of Beijing.

J. Wang
LASG, Institute of Atmospheric Physics,
Chinese Academy of Sciences,
Beijing 100029, China

J. Wang
Graduate School of Chinese Academy of Sciences,
Beijing 100049, China

R. Zhang
State Key Laboratory of Severe Weather,
Chinese Academy of Meteorological Sciences,
Beijing 100081, China

Y. Wang
Institute of Urban Meteorology,
China Meteorological Administration,
Beijing 100089, China

R. Zhang (✉)
Chinese Academy of Meteorological Sciences,
No.46 Zhong-Guan-Cun South Avenue, Haidian District, Beijing 100081, China
e-mail: renhe@cams.cma.gov.cn

1 Introduction

Local precipitation patterns affected by urbanization have been studied intensively. Many earlier studies that focused on the effects of urban expansion on rainfall amount and frequency indicated that the seasonal or daily precipitation amount and frequency over urban and downstream areas were significantly larger than those over surrounding areas (Changnon 1968; Huff and Changnon 1972, 1973; Huff and Vogel 1978; Balling and Brazel 1987; Jauregui and Romales 1996; Shepherd et al. 2002; Burian and Shepherd 2005; Shepherd

2006; Mote et al. 2007). These regional differences were especially remarkable between noon and midnight during days of intense rain in the warm season, and showed an intensifying trend in response to rapid urbanization (Huff and Changnon 1973; Huff and Vogel 1978; Burian and Shepherd 2005). Urban growth is commonly associated with increased rainfall in urban and downwind areas because of the establishment of a convergence zone related to the urban heat island effect (e.g., Bornstein and Lin 2000; Baik et al. 2001; Rozoff et al. 2003; Burian and Shepherd 2005). In contrast, other studies have reported declines in rainfall during extended periods of strong urban growth because of high concentrations of anthropogenic aerosols in small cloud droplets, which acts to suppress drop coalescence and the rain process (Rosenfeld 2000; Ramanathan et al. 2001; Andreae et al. 2004; Givati and Rosenfeld 2004; Khain et al. 2005).

The Beijing metropolitan region is located in Northern China and is one of the largest megacities in the world, with a population of more than 18 million. The city has expanded rapidly in recent decades, resulting in significant modifications to surface properties and local atmospheric circulations. Therefore, studies of temporal and spatial variations in the local climatic characteristics of Beijing are important to our understanding of the impacts of urbanization on local climate. Miao et al. (2009) modeled the impacts of urban land use on the characteristics of boundary layer structures, and revealed that urban–rural circulations induced by topographic differences are an important cause for the prevalence of mountain–valley flows in Beijing. Zhang et al. (2009) used a mesoscale model to simulate rainfall events and found that urban expansion contributed to a reduction in precipitation over the Beijing area, particularly over the Miyun reservoir area. Moreover, Beijing has a varied and complex topography, with high mountains to the west (Taihang Mountains), north, and northeast (Yan Mountains), accounting for approximately three quarters of the Beijing metropolitan region; consequently, the terrain has an important effect on the location and distribution of precipitation in Beijing (Zhang et al. 2005). Sun and Yang (2008) studied the summer meso-β scale rain in Beijing and found it was caused by the joint effects of topography and the urban heat island. They reported the formation of a strong temperature gradient that engendered a wind shear near windward slopes, because the terrain blocked the horizontal diffusion of heat generated by the heat island effect. This wind shear is important in developing and maintaining the convection; consequently, most of the mesoscale rain processes in Beijing occur at the margin of the urban area or in adjacent mountainous areas (Sun et al. 2006; Sun and Yang 2008; Wu et al. 2009).

Beijing has a typical monsoonal climate, and summer precipitation is the main source of water (Zhang et al. 2009). Diurnal variations in precipitation, which are important for the hydrological cycle and agriculture, have a strong influence on the local weather and global climate (Dai 2001; Zhou et al. 2008; He and Zhang 2010). Li et al. (2008) investigated diurnal variations in precipitation over Beijing using data from a single representative meteorological station, and found that both rainfall amount and frequency were high from the late afternoon to the early morning, with minima around noon.

Given the complex terrain and surface features within the Beijing metropolitan region, it is insufficient to study diurnal variations in meteorological factors using data from a single station. With the rapid development of a meteorological observation network in Beijing, real-time data with high temporal resolution have become available, enabling analyses of diurnal cycles of meteorological factors over urban, suburban, and mountainous areas. By using observations at 20 stations in Beijing and 6 stations in neighboring Hebei Province, Yin et al. (2011) investigated diurnal variations of precipitation frequency and pointed out their differences in different locations of the observing stations in Beijing. They explained the differences of the diurnal variations by the mountain–valley circulation and urbanization. However, in order to understand the precipitation diurnal variations in different areas in Beijing, an objective division of the Beijing metropolitan region is needed. Moreover, the thermal effect of the urban, suburban and mountainous areas of Beijing on local circulations responsible for the precipitation diurnal variations should also be investigated. The study of Yin et al. (2011) dealt with only the diurnal variations of precipitation frequency. It is also important to understand the diurnal variations of precipitation amount and intensity in the different areas in Beijing.

The present study investigates the differences in diurnal variations of precipitation amount, frequency and intensity between areas with distinct land use and topography, and explores the reasons for such differences, considering topographic and urbanization effects. The remainder of the manuscript is organized as follows. In Section 2, we describe the data and the method employed in our analysis. In Section 3, we describe the division of Beijing into four areas according to the underlying surface conditions and the climatic characteristics of summer precipitation. Section 4 presents a discussion on the differences in diurnal variations in the amount, intensity, and frequency of precipitation over the four areas. Diurnal profiles of the normalized amount, intensity, and frequency of precipitation are provided in Section 5, along with their spatial distributions. In Section 6, we explore the origin of these patterns from the perspective of the local atmospheric circulation. Finally, the conclusion and discussion are presented in Section 7.

2 Data and methods

We utilize hourly rain-gauge data, hourly 10-m wind-field data, and hourly 2-m air-temperature data for summer (June–August) in 2004–2007, as well as daily rain-gauge

data, 2-m air-temperature data, and 2-m relative humidity data at 6-h intervals for summer in 1991–2007, sourced from 20 routine meteorological stations in Beijing operated by the Beijing Meteorological Bureau of the China Meteorological Administration. The 20 stations are as follows: Haidian (HD), Chaoyang (CY), Fengtai (FT), Shunyi (SY), Tongxian (TX), Daxing (DX), Nanjiao (NJ), Mentougou (MTG), Fangshan (FS), Changping (CP), Shijingshan (SJS), Miyun (MY), Shangdianzi (SDZ), Huairou (HR), Pinggu (PG), Tanghekou (THK), Yanqing (YQ), Foyeding (FYD), Zhaitang (ZT), and Xiayunling (XYL), and their locations are shown in Fig. 1.

The hourly rain-gauge data for 2004–2007 are selected for analyses because the stations were well maintained during these years. All the data met strict quality-control standards required by the Rules on Ground Surface Meteorological Observations (China Meteorological Administration 2003) and were collected uniformly at each of the 20 stations. We also conducted quality-control procedures to identify anomalous observations of hourly rainfall data, based on the thresholds proposed by Ren et al. (2010). The proportion of missing hourly rainfall data during 2004–2007 is less than 0.1 % for 19 stations, and 5.6 % for FT station, representing an overall low rate of missing data for the study period. We also checked for erroneous 2-m temperature data based on upper and lower thresholds of 60 °C and −80 °C (Dou et al. 2008), respectively.

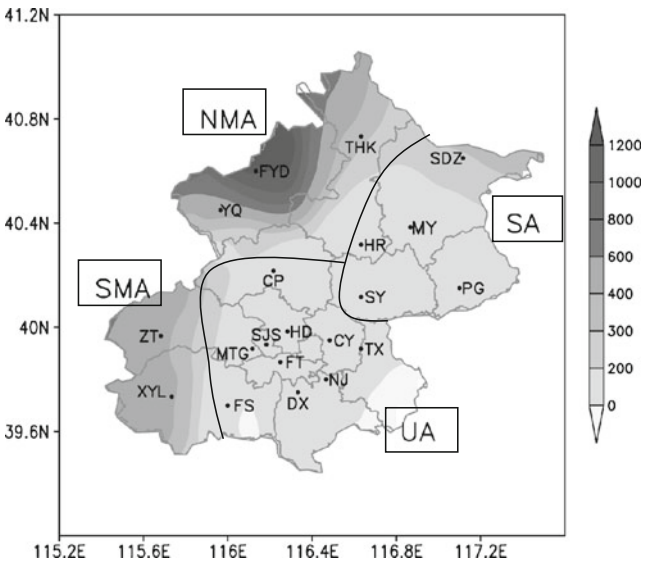

Fig. 1 Distribution of 20 meteorological stations in Beijing. *Solid lines* denote the boundaries of the four areas. UA, SA, NMA, and SMA refer to the urban area, the suburban area, the northern mountainous area, and the southern mountainous area, respectively. The 20 stations are HD (Haidian), CY (Chaoyang), FT (Fengtai), SY (Shunyi), TX (Tongxian), DX (Daxing), NJ (Nanjiao), MTG (Mentougou), FS (Fangshan), CP (Changping), SJS (Shijingshan), MY (Miyun), SDZ (Shangdianzi), HR (Huairou), PG (Pinggu), THK (Tanghekou), YQ (Yanqing), FYD (Foyeding), ZT (Zhaitang), and XYL (Xiayunling). The shading represents elevation (unit: in meters)

For wind direction and speed, the thresholds were 0°–360° and 0–75 m/s (Dou et al. 2008), respectively.

According to the Rules on Ground Surface Meteorological Observations (China Meteorological Administration 2003), precipitation amounts less than 0.05 mm are recorded as 0.0 mm, and amounts greater than 0.05 mm but less than 0.1 mm as 0.1 mm. In this study, a threshold rate of 0.1 mm h^{-1} is specified to define a precipitation event, because the data are only accurate to one decimal place.

The precipitation frequency refers to the number of occurrences of predefined precipitation events. We use the definition of precipitation intensity given by Oke and Musiake (1994), as follows:

$$I(h) = \frac{P(h)}{N(h)} \tag{1}$$

where $P(h)$ is the total amount of rainfall and $N(h)$ is the total number of precipitation events at time h at a station.

To compare diurnal variations in precipitation at different areas in the same hour or period, the amount, intensity, and frequency of precipitation are normalized to the seasonal averages of 20 stations for each hour, based on the following formula:

$$A_{h,s} = \frac{P_{h,s} - W_h}{W_h} \times 100\% \tag{2}$$

where $A_{h,s}$ is the hourly normalized precipitation amount (or intensity, or frequency) at time h (h=0, 1, 2, … 23) and at station s (s=1, 2, … 20); $P_{h,s}$ is the seasonal average precipitation amount (or intensity) or total number of occurrences at time h and at station s; and W_h is the mean precipitation amount (or intensity or total number of occurrences) at the 20 stations at time h. The amount, intensity, and frequency of precipitation are also normalized to the daily average of the 20 stations throughout Beijing, using the following formula:

$$B_{h,s} = \frac{P_{h,s} - X}{X} \times 100\% \tag{3}$$

where $B_{h,s}$ is the daily normalized precipitation amount or intensity at time h and at station s, and X is the averaged daily average amount or intensity of precipitation at the 20 stations.

To divide the Beijing metropolitan region into different areas characterized of distinct topographic conditions, we first use an empirical method in terms of the distinct characteristics of urban, suburban, and mountainous areas. In addition to the empirical method, we also use a varimax-rotated empirical orthogonal function (REOF) analysis (Richman 1986), based on the precipitation features, to verify the empirical geographic division. The REOF mode refers to a linear transformation of the initial empirical orthogonal function (EOF) mode, using the varimax method. The varimax method maximizes the variance of the squared correlation coefficients between the

time series of each REOF mode and the original time series. In this way, the loadings of the REOF modes are widely distributed, with a few large loadings and many others close to zero. Hence, REOF analysis reveals simple patterns and increases the discrimination among the loadings, making them easier to interpret. The usefulness of REOF analysis in revealing the spatiotemporal variability of an anomaly pattern had been well documented in previous studies (e.g., Horel 1981; Richman 1986).

Using the method proposed by Zhou et al. (2008), we interpolate summer precipitation and 10-m wind data from the 20 stations into gridded precipitation and winds at 0.1° latitude×0.1° longitude, to calculate the REOF and divergence, respectively. Since the 10-m wind is not in the same level at different stations, the 10-m height above the ground surface can be recognized as a sigma surface and the divergence can be calculated in the terrain following coordinate (Dai and Deser 1999). Therefore, we use the finite difference method of Dai and Deser (1999) to calculate the horizontal divergence from interpolated gridded winds. The time used in this study is Beijing local standard time (LST), and summer refers to the months of June, July, and August (JJA).

3 Geographic divisions

Based on underlying surface conditions, Beijing is empirically divided into four areas: the urban area (UA), suburban area (SA), north mountainous area (NMA), and south mountainous area (SMA) (see Fig. 1). Urban growth during the 1980s has seen several suburban areas become connected to the central city (Wang et al. 2007), so we define the area within the Sixth Ring Road as UA, which includes 10 stations and covers the districts of HD, CY, SJS, NJ, FT, TX, DX, MTG, FS, and CP. Northeast Beijing has experienced a slower rate of urban growth and is located far from the central city, consequently, it is defined as SA, which includes the districts of MY, SDZ, HR, and PG. Considering the distinctive climatic features of the mountains and the plain, we classify the districts of THK, YQ, and FYD, with altitudes of 333.7 m, 489 m, and 1,216.9 m, respectively, as NMA. The districts of ZT and XYL, at altitudes of 441.1 m and 409 m, respectively, are defined as SMA.

To verify the credibility of the empirical division described above, which is based on underlying surface conditions, the REOF method is applied to analyze the summer precipitation data matrix for 17 summers (1991–2007) at the 20 stations. The cumulative contributions of the first three leading modes revealed by the REOF analysis account for 87.7 % of the total variance, so we select the first three modes to be rotated. The rotated eigenvectors reveal good spatial separation (Fig. 2): high loadings are concentrated in the northeastern areas (including SDZ, MY, PG, HR, and SY), in the southwestern areas (including XYL, ZT, and FS), and in the northwestern areas (including THK, YQ, FYD, and CP), and these areas are referred to as REOF 1 (as shown in Fig. 2a), REOF 2 (as shown in Fig. 2b), and REOF 3 (as shown in Fig. 2c), respectively. The spatial distributions of the three independent areas with high loadings, as indicated by the REOF technique, agree with our empirical division, with REOF 1, REOF 2, and REOF 3 corresponding to SA, SMA, and NMA, respectively. This result demonstrates the credibility of the empirical regional division. However, it must be noted that the central Beijing area is not included in the areas described above, which indicates that variation in summer precipitation over central Beijing differs from that over the other three areas. Taking into account the distribution of geographic features in Beijing, we classify the central area as UA.

There are, however, two contradictions between the empirical and REOF division results. First, as shown in Fig. 1, FS and CP belong to UA according to the empirical division results, but they are not included in UA by the REOF method, as shown in Fig. 2b and c, respectively. This discrepancy may have resulted from a spatial interpolation error when we interpolated the station data to grids. To obtain a more reliable result, correlation analysis was applied, and the correlation coefficients between FS and the other nine urban stations, calculated for hourly and daily precipitation, 6-h temperature, and relative humidity, are significantly higher than those between FS and the suburban or mountainous stations. Similarly, CP has a stronger relationship with the other nine urban stations than does with the NMA stations, as shown in Table 1, which summarizes the correlation coefficients between FS (or CP) and other areas. Second, although SDZ is located in a mountainous area with an elevation of 286.5 m, its REOF result and its strong relationship with suburban stations (Table 1) indicate that SDZ should be included in SA, as shown in Fig. 2a, rather than in the mountainous areas.

4 Amount, intensity, and frequency of precipitation

In order to investigate the features of precipitation over the four areas, in Fig. 3 we show diurnal variations in 3-h moving averages of the seasonal hourly mean amount (Fig. 3a), intensity (Fig. 3b) and frequency (Fig. 3c) of precipitation over each of the four areas outlined in Fig. 1.

4.1 Precipitation amounts

As shown in Fig. 3a, UA has a peak precipitation amount at 1900 LST. NMA and SMA show a maximum at around 1800 and 1700 LST, respectively, 1 and 2 h earlier than UA. SA shows two peaks in precipitation amount: the first peak is consistent with that at UA, and the second, weaker peak occurred at around 0600 LST. There are also two peaks at

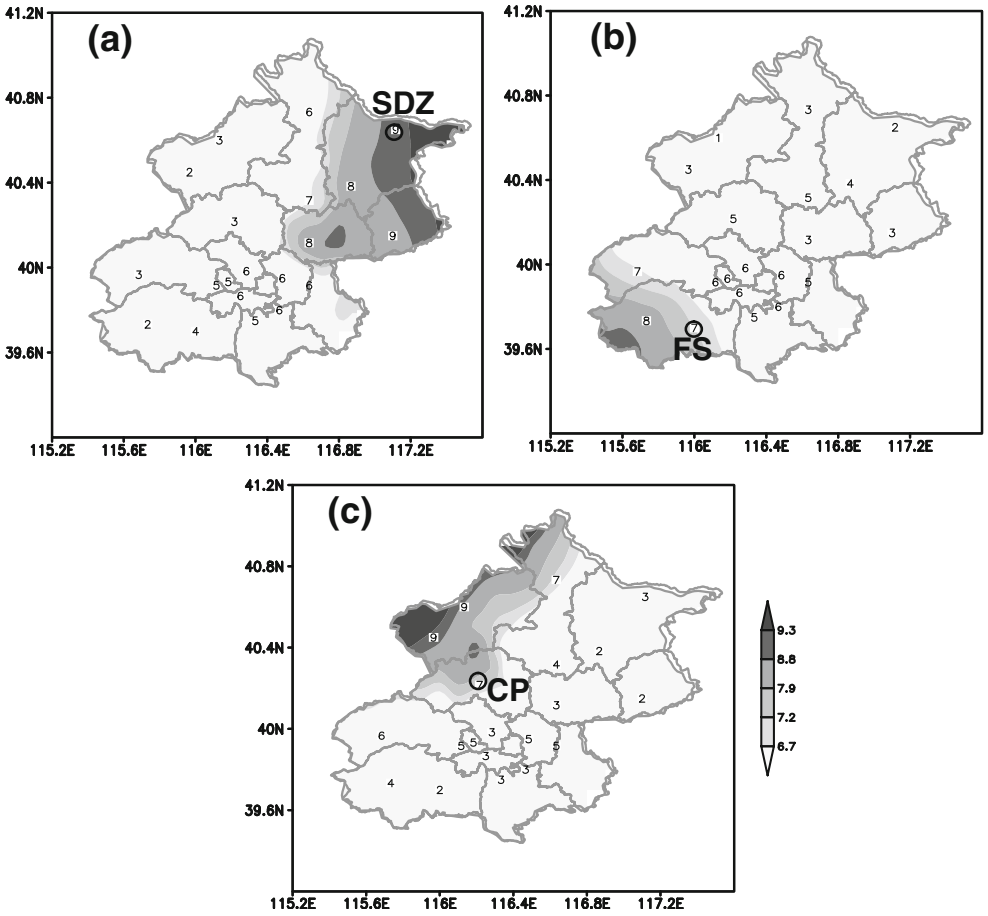

Fig. 2 **a** REOF 1 for the average amount of precipitation in 1991–2007 summers (JJA). **b** and **c** As for **a** but for REOF 2 and REOF 3. The *circles* denoted by SDZ, FS, and CP refer to the locations of Shangdianzi, Fangshan, and Changping, respectively. The *numerals* in each plot are REOF loadings multiplied by 10. Loadings larger than 0.67 are *shaded*

SMA, with the weaker nocturnal diurnal peak appearing at around 0100 LST.

The minimum amounts of precipitation over the four areas are all observed in the morning. NMA has the earliest minimum at around 0900 LST, followed by SMA at around 1000 LST, and UA and SA at around 1100 LST. In terms of daily precipitation amount, SA has the greatest amount of 8.09 mm, followed by UA with 7.09 mm. By checking each station in both SA and UA, we confirmed that the daily precipitation amount at each of four stations (MY, HR, SY, and PG) out of five in SA is larger than that at each of nine stations out of ten in UA, with only one station, SDZ, in SA and one, MTG, in UA having less daily precipitation amount of 7.48 mm and more amount of 8.90 mm, respectively. The fact that SA records the largest precipitation amount may reflect urban effects that enhance rainfall in the downwind area of UA (Changnon 1968; Huff and Changnon 1972; Rozoff et al. 2003; Diem and Brown 2003; Shepherd 2006), since the winds are primarily southerly during summer in Beijing (Sun and Shu 2007).

Table 1 Correlation coefficients of hourly and daily precipitation amount, 6-h temperature and relative humidity at FS compared with UA and SMA, at CP compared with UA and NMA, and at SDZ compared with SA and NMA

Station	Area	Hourly	Daily	Temp.	Humidity
FS	UA	0.28	0.69	0.995	0.995
	SMA	0.25	0.67	0.995	0.865
CP	UA	0.25	0.65	0.993	0.992
	NMA	0.24	0.62	0.981	0.911
SDZ	SA	0.30	0.66	0.999	0.998
	NMA	0.16	0.53	0.993	0.899

The periods of hourly and daily precipitation amount are 2004–2007 and 1991–2007, respectively

To test for the statistical significance of differences in diurnal variations over the four areas, an F test is applied to assess whether the standard deviations of the precipitation amounts over any two areas differ from each other. The amounts of hourly precipitation in the summers (JJA) of 2004–2007 are compared among UA, SA, NMA, and SMA. All the results pass the F test at the 1–2 % significant level, indicating significant differences in diurnal variations in precipitation amount in the four areas. The F test results and corresponding p values are listed in Table 2. Here we can see, without considering the individual diurnal variation in precipitation amount at each station in each area, the area

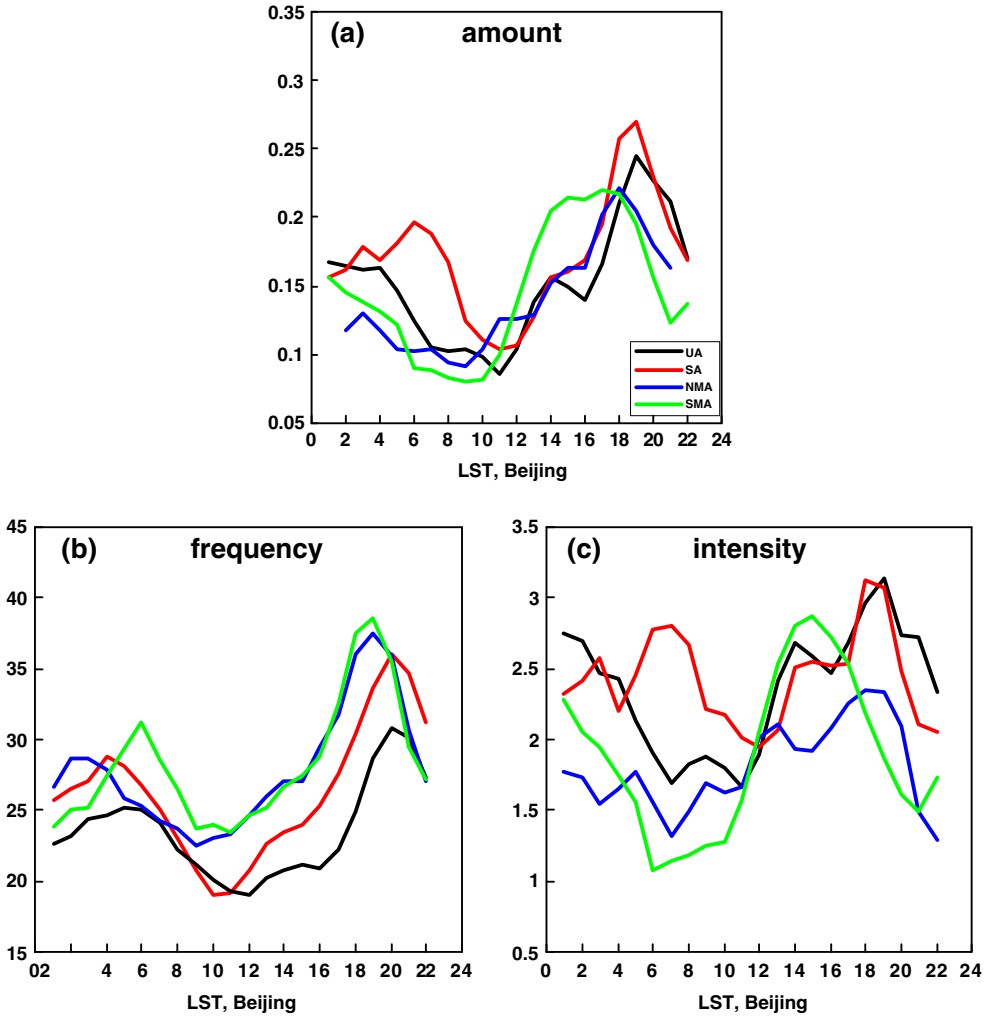

Fig. 3 2004–2007 summer mean diurnal variations in **a** precipitation amount (unit: in millimeters per hour), **b** precipitation frequency (unit: number of occurrences), and **c** precipitation intensity (unit: in millimeters per hour) averaged over UA, SA, NMA, and SMA. The amount, intensity, and frequency of precipitation are 3-h moving averages of hourly data

mean differs significantly from each other among the four areas.

4.2 Frequency and intensity of precipitation

Figure 3b shows that the diurnal profiles of precipitation frequency over the four areas are basically identical, with a dominant peak in the evening and a secondary peak in the early morning, which are similar to the results of Yin et al. (2011). Precipitation over UA and SA occur most frequently at around 2000 LST, later than those over NMA and SMA, where the most frequent rainfall events are observed at around 1900 LST. The secondary frequency peaks in UA and SMA occur at around 0600 LST, whereas the weaker frequency peaks in NMA and SA occur at around 0200 and 0400 LST, respectively.

We estimated the mean intensity of precipitation using Formula (1). As shown in Fig. 3c, UA and NMA have a single intensity peak, which occurs at around 1900 LST, whereas SMA reaches its peak intensity at about 1500 LST, earlier than the other three areas. In contrast, two peaks in precipitation intensity are observed in SA, at around 1900 LST and 0700 LST. The precipitation intensity in SMA shows a minimum at an earlier time than in the other areas, at about 0600 LST, followed by the minimum intensity in NMA at 1 h later; the minimum precipitation intensity at UA and SA occur at around 1100 and 1200 LST, respectively.

Comparing Fig. 3c with Fig. 3a, the diurnal variation in precipitation intensity is basically identical to the diurnal variation in the amount of precipitation. To compare the relative contributions of the diurnal cycles of the precipitation frequency and intensity to that of precipitation amount, we estimated the percentage variance of diurnal cycle of rainfall amount accounted for by the precipitation frequency and intensity, respectively, by using the method of Zhou et al. (2008). For the four areas of UA, SA, NMA and SMA, the precipitation intensity accounts for 77.7, 65.5, 78.7 and 79.6 %, respectively, while the frequency accounts for 45.3, 39.2, 64.1, and 11.8 %, respectively. The contribution from the precipitation intensity is clearly larger than that from the frequency in each of the four areas. Therefore, the diurnal variation of intensity is more identical to that of amount.

Table 2 Significance level (p value) of the F test using hourly precipitation amount in 2004–2007 summers between each pair of UA, SA, NMA, and SMA

	UA–SA	UA–NMA	UA–SMA	SA–NMA	SA–SMA	NMA–SMA
p value	0.001	0.001	0.011	0.001	0.022	0.001

4.3 Peak time of precipitation amounts

Figure 4 shows the spatial distribution of the times of peak precipitation amount (T_{max}, in hours) at the 20 stations. The prevailing evening and midnight maximum precipitation at UA is clearly identifiable, whereas there is no maximum in the morning, which is in accordance with the above findings (Fig. 3a). Two precipitation peaks are observed in SA: in the morning and in the evening. We calculated quantitatively the precipitation amount. In western SA (MY, HR, SDZ, and SY), the peak precipitation amount at 1900 LST is 0.31 mm h^{-1}, while that at 0700 LST is 0.19 mm h^{-1}. At PG, the peak precipitation amount at 1900 LST is 0.29 mm h^{-1} and that at 0700 LST is 0.32 mm h^{-1}. Therefore, western SA has a greater amount of rainfall at the evening peak (1900 LST), whereas the PG station (in southeastern SA) has more precipitation at the morning peak (0700 LST) than that at the evening peak, which implies that the peak time is different in different parts of SA. A single late-afternoon precipitation peak prevails in NMA, earlier than almost all peak times in UA except that at FT where the peak time appears around 1800 LST, about 1 h earlier than those in NMA. Although T_{max} at XYL is later, SMA has the earliest peak, which may be attributable to the propagation of local precipitation from west to southeast over North China (He and Zhang 2010), resulting in the earliest precipitation peak over ZT and a later maximum over XYL.

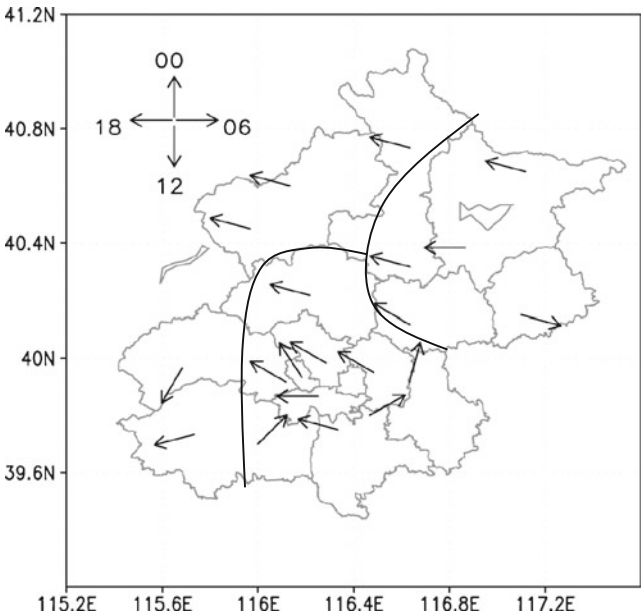

Fig. 4 Spatial distribution of the times of peaks in precipitation amount at 20 stations in Beijing. The unit vectors denote Beijing local standard time (LST), as shown in the phase clock at the *top left*. The four areas are separated by *solid lines*

5 Normalized amount, intensity, and frequency of precipitation

Because precipitation is related to topography, latitude, and underlying surface conditions, normalized precipitation is more suitable for assessing differences in precipitation over different areas in Beijing. Therefore, we normalized the precipitation by its hourly and daily means for the whole Beijing region according to Formulas (2) and (3), respectively, in order to compare the precipitation differences among the four areas.

5.1 Normalized precipitation amount

Figure 5a shows diurnal variations in the normalized precipitation amount based on Formula (2). In the morning, the amount of precipitation in SA accounts for the highest ratio of the total precipitation amount among the four areas, exceeding 47.1 % of the hourly average precipitation amount over the whole region of Beijing at around 0700 LST, which corresponds to its morning peak. UA has an amount equivalent to the average during the morning period. In contrast, the mountainous areas account for the lowest ratio. For example, the ratio of NMA is 21.9 % lower than the average at around 0700 LST, which corresponds to its minimum in the morning. In the afternoon, SMA accounts for the highest ratio, which is 32.1 % higher than the average at 1500 LST, corresponding to its afternoon maximum. After 1900 LST, UA presents a larger precipitation amount than the average, and a maximum percentage of 30.1 % higher than the average appears at 2100 LST. The amount of precipitation in SA also increases in the evening, and is 21.6 % higher than the average at 1900 LST, corresponding to its evening peak. Although NMA shows a rainfall peak in the evening, its ratio to the average is relatively low (around zero) because the amount of precipitation is less than those at UA and SA. SMA has the smallest amount of precipitation in the evening, and the ratio is 34.2 % lower than the average at the minimum at 2000 LST.

5.2 Normalized intensity and frequency of precipitation

The same technique was used to assess diurnal variations in precipitation intensity in the four areas, as well as areal differences. Figure 5b shows that the diurnal variation patterns of rainfall intensity resemble those for rainfall amount (Fig. 5a). In particular, SA has the strongest rainfall intensity, with a ratio to the average of the hourly precipitation intensity for the whole region of Beijing exceeding 45.2 % at 0700 LST, while the intensity at UA is equivalent to the average. In contrast, the mountainous areas have weaker intensities. For example, the ratio of SMA is 39.1 % lower than the average at 0600 LST, although it increases and accounts for the highest ratio at around 1500 LST, being 15.6 % higher than the average. NMA shows the weakest intensity, with its lowest ratio being 37.4 % weaker than the average at about 2100 LST. From the late afternoon to evening, the precipitation intensity in UA increases and it exceeds the average by 19.7 % at 2100 LST.

Figure 5c shows diurnal variations in the hourly normalized precipitation frequency in the four areas, based on Formula (2). In the mountainous areas, it rains most frequently in the daytime (0800–2000 LST). In particular, both SMA and NMA have frequency peaks at 1800 LST, with a ratio to the average of the hourly total number of occurrences in the whole region of Beijing, of 34.1 % in SMA and 28.2 % in NMA, which correspond to their evening maximum precipitation frequency. A frequency of 14.1 % higher than the average is observed in SA at 2100 LST. However, the precipitation frequency in UA is the lowest throughout the day, especially during the late-afternoon period, when the ratio is 16.8 % lower than the average at its minimum at about 1800 LST. The second highest frequencies are observed in SA and the mountainous areas during 0200–0600 LST, which corresponds to their secondary peaks (Fig. 3b). Taking into account the diurnal variations in precipitation intensity, the amount of precipitation in UA remains at a low level because of its lower frequency, despite its strong intensity, which is consistent with

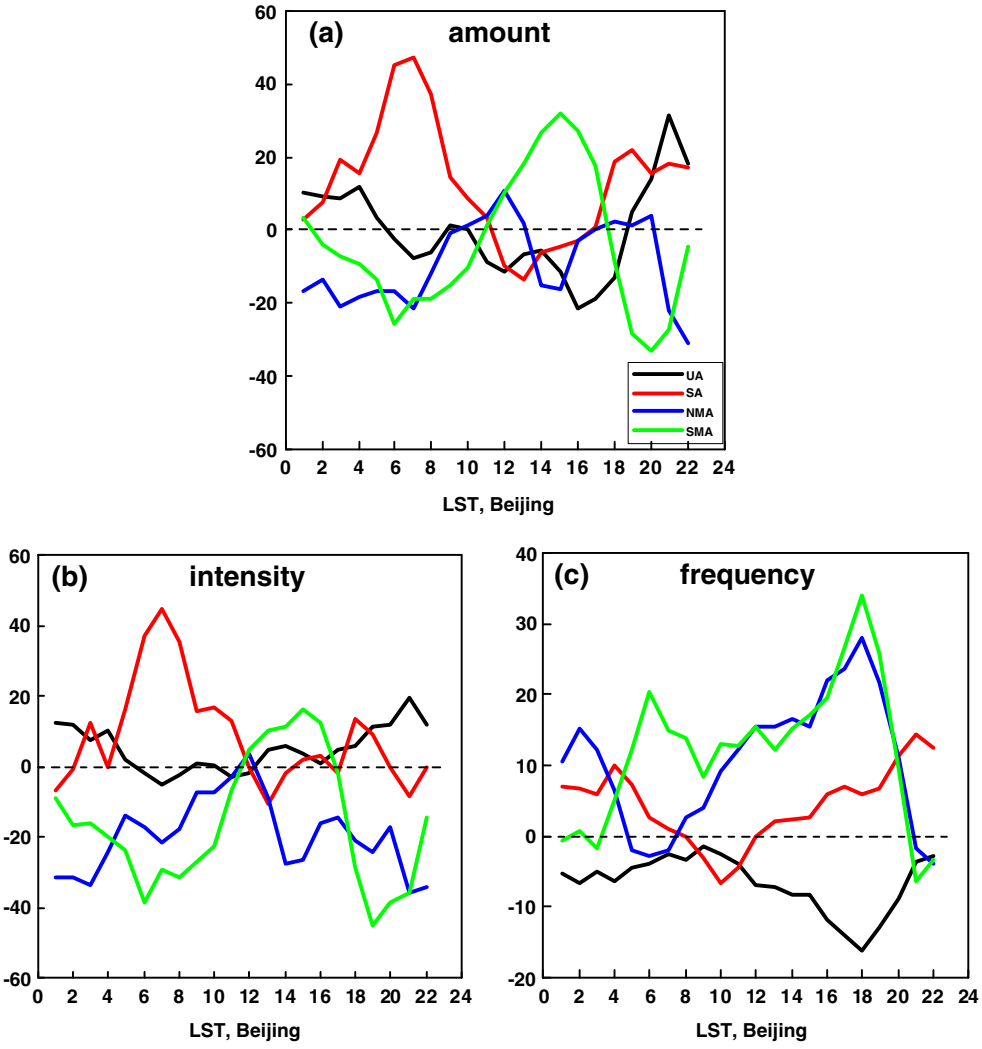

Fig. 5 2004–2007 summer mean diurnal variations in normalized precipitation **a** amount, **b** intensity, and **c** frequency in the four areas marked in Fig. 1 (unit: in percent). All data are 3-h moving averages

previous reports (e.g., Dai et al. 2007; Zhou et al. 2008) that diurnal variation in the amount of rainfall is influenced by both rainfall frequency and intensity.

5.3 Spatial distribution of the normalized amount and intensity of precipitation

Spatial patterns are important in terms of verifying precipitation features over UA, SA, and the mountainous areas. Therefore, we select 0500–0800 LST, 0900–1200 LST, 1400–1700 LST, 1800–2100 LST, and 0100–0400 LST as five representative periods, considering that the maximum and minimum amounts, and intensities of precipitation over the four regions occur mainly during these periods. Figure 6 shows the spatial distributions of the normalized amount (Fig. 6a, c, e, g, i) and intensity (Fig. 6b, d, f, h, j) of precipitation, calculated as percentages of anomalies relative to the daily mean of the 20 stations, based on Formula (3). In terms of the regional average, the largest amounts (Fig. 6a) and intensities (Fig. 6b) of precipitation occurred in SA and at individual urban stations in the southeast at around 0500–0800 LST, whereas the amounts and intensities are lowest in the western UA and the mountainous areas. During 0900–1200 LST, almost all four areas have negative percentages except the small area in southern SA for the amounts (Fig. 6c) and intensities (Fig. 6d) of precipitation. For example, UA and SA show minimum amounts and intensities of precipitation during this period compared with the other four periods. The amount (Fig. 6e) and intensity (Fig. 6f) of rainfall in SMA reach a peak during the 1400–1700 LST period, when the amounts and intensities of precipitation over the western UA, southwest SA, and NMA gradually increase. During 1800–2100 LST, the amounts (Fig. 6g) and intensities (Fig. 6h) of rainfall show a peak in UA, SA, and NMA, whereas the amount and intensity of rainfall in SMA show a decrease. Although the precipitation amount (Fig. 6i) decreases in UA and SMA during 0100–0400 LST compared with 1800–2100 LST, the precipitation amount in SMA is still larger than that during 0500–0800 or 0900–1200 LST, which corresponds to its secondary peak. The rainfall intensity over SMA (Fig. 6j) also shows a secondary peak during 0100–0400 LST and is stronger than those during other periods, except the peak during 1400–1700 LST. SA presents strong centers for both rainfall amount and intensity during 0100–0400 LST which are similar but weaker comparing to those during 0500–0800 LST, when the secondary peak is observed over SA. These observations of diurnal variations in precipitation indicate that UA in Beijing does not have a significantly greater amount of rainfall, or stronger intensity or higher frequency, than SA or the mountainous areas, especially during the daytime, which contradicts the findings of previous studies (e.g., Huff and Changnon 1972; Huff and Vogel 1978).

6 Physical interpretations

To explore why the diurnal variations in precipitation differ among UA, SA, and the mountainous areas, hourly 10-m wind-field data and 2-m temperature data from the 20 stations are used to investigate the characteristics of local circulations induced by the inhomogeneity of thermal conditions at the underlying surface, which could be attributable to topographic effects and land use differences.

Figure 7 shows temporal variations in 2-m temperature anomalies at UA, SA, SMA, and NMA, respectively. The temperature anomalies are calculated by subtracting the daily averaged temperature of the 20 stations from the mean temperature in each area at each hour. Consistent diurnal variations in the temperature anomalies are demonstrated in the four areas, which peak at around 1500 LST, with a minimum at 0500 LST. Nevertheless, there are significant differences between the values for the temperature anomalies: the highest is observed in UA, SA has a smaller temperature anomaly, and NMA has the smallest for the whole day. Moreover, UA shows a positive temperature departure after 0800 LST, whereas SA and SMA show positive temperature anomalies about 1 h later, and NMA lags UA by about 4 h. UA does not show a negative anomaly until 2300 LST, whereas SA and the mountainous areas show negative anomalies 2–5 h earlier than this time. The higher temperature and longer period of positive anomalies in UA may reflect the sparse vegetation coverage and large numbers of buildings and sealed roads, which trap short-wave radiation and store heat during the daytime to a greater degree than other land covers, releasing the heat from the ground to the air at night in the form of long-wave radiation to generate warmth (Voogt 2004; Miao et al. 2009). Anthropogenic heat may also contribute to the heat island effect (Sailor and Lu 2004; Voogt 2004; Miao et al. 2009). Besides, the highest temperature in UA could also reflect its relatively low elevation (Chemel et al. 2007).

In order to investigate the influence of the underlying surface differences among different areas on the local circulation and precipitation, Fig. 8 shows the average diurnal variations of the divergence in each area, in which negative and positive values indicate convergence and divergence, respectively, calculated from hourly 10-m wind-field data from the 20 stations. Variations of the divergence are consistent with those for precipitation, as shown in Fig. 6. UA and SA show stronger convergence during 0100–0400 and 0500–0800 LST, when more precipitation occurs, whereas the mountainous areas show less precipitation (see Fig. 6i, a). During 0900–1200 LST, divergence fields appear in UA and SA, where the positive precipitation anomalies disappear and negative anomalies develop. At this time, convergence fields become stronger in the mountainous areas, where precipitation increases with a significant decrease in negative precipitation anomalies compared with 0500–0800 LST (see Fig. 6c). For

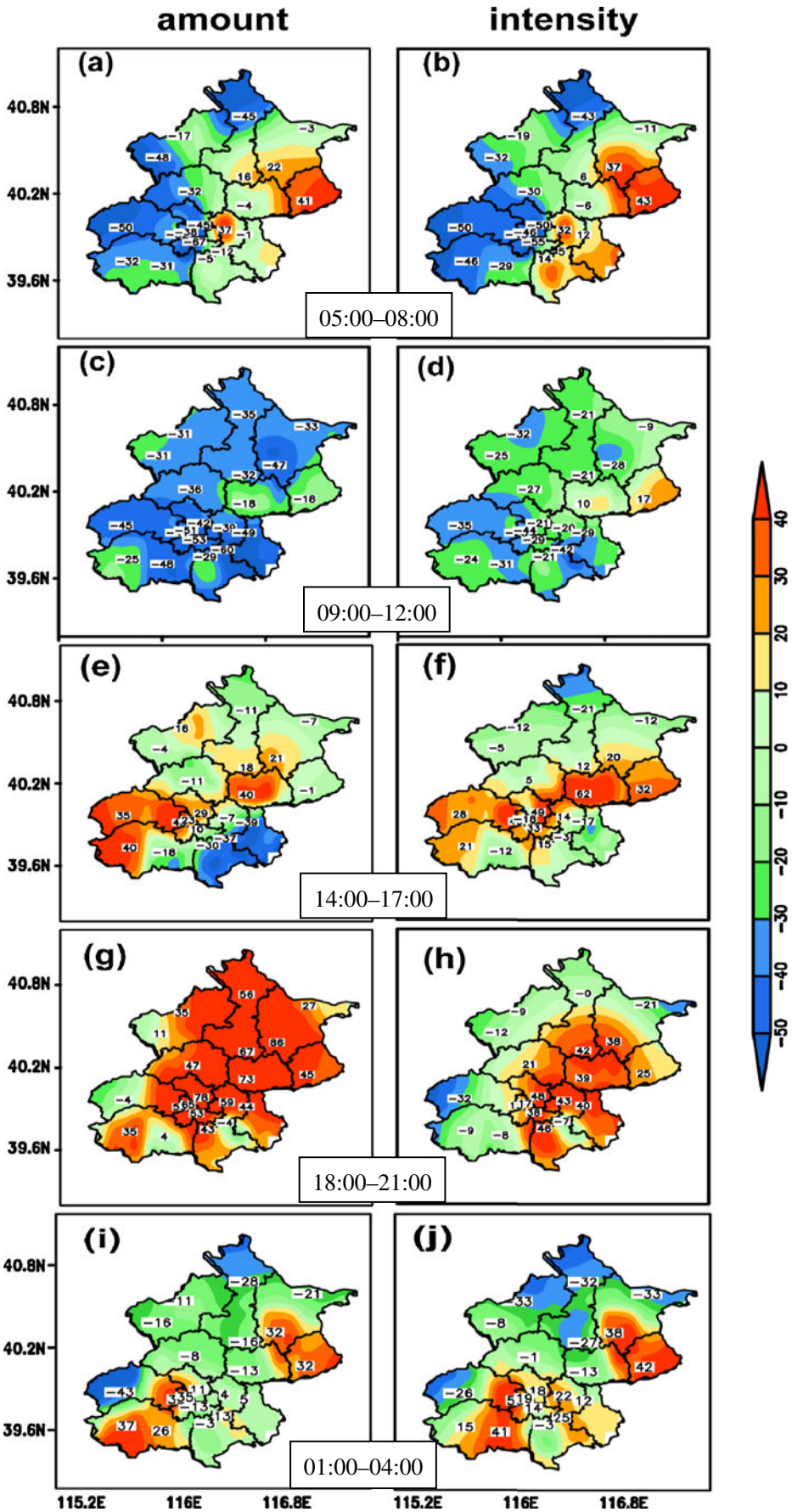

Fig. 6 Spatial distribution of the normalized amount (*left panel*) and intensity (*right panel*) of precipitation, calculated as percentages of anomalies relative to the daily means in summer (2004–2007) for the whole Beijing area (unit: in percent), averaged for the periods **a** and **b** 0500–0800 LST, **c** and **d** 0900–1200 LST, **e** and **f** 1400–1700 LST, **g** and **h** 1800–2100 LST, and **i** and **j** 0100–0400 LST

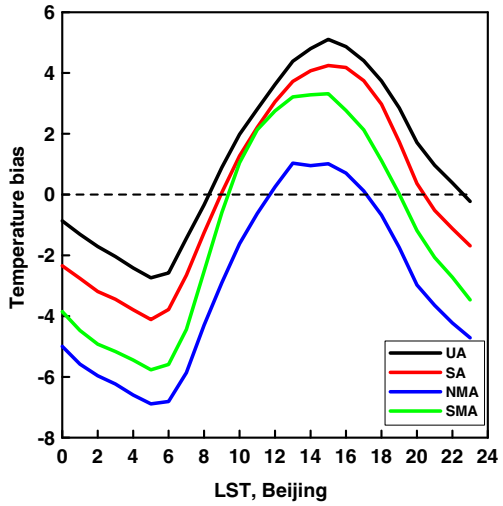

Fig. 7 Diurnal variations in seasonal mean temperature anomalies relative to the daily average for the 20 stations (unit: in degrees Celsius) in UA, SA, NMA, and SMA

the period 1400–1700 LST, UA and the mountainous areas all generate convergence, and the divergence in SA is weakened. Accordingly, positive precipitation anomalies are observed along the regions from the southwest to the northeast, and the negative anomalies in other areas are significantly reduced, as shown in Fig. 6e. During 1800–2100 LST, convergence fields dominate the four regions and positive rainfall anomalies are observed in almost all areas, as shown in Fig. 6g.

A comparison of Figs. 7 and 8 reveals that although the temperature increases earlier and to a greater extent in UA and SA, no convergence field is induced by surface heating. Instead, the formation of divergence fields may be related to the local mountain–valley circulation. To show variations in mountain–valley breezes, diurnal variations in surface 10-m

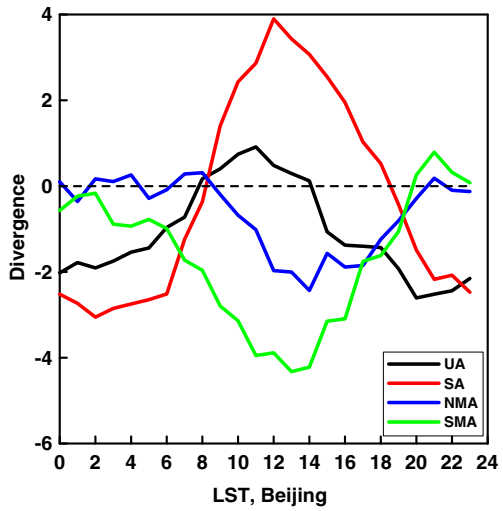

Fig. 8 Diurnal variations in divergence averaged over UA, SA, NMA, and SMA. Positive and negative values represent divergence and convergence (unit: 10^{-5} per second), respectively

winds are plotted in Fig. 9. In the early afternoon (1400 LST) and in the evening (2000 LST), southerly valley winds are widespread over most of the Beijing metropolitan region. During the late night (0200 LST) and early morning (0800 LST), in contrast, northerly mountain winds are dominant. The distributions of the winds shown in Fig. 9b and d are similar to the observed surface winds at 0800 LST and 2000 LST, respectively, as shown by Yin et al. (2011).

From morning to noon, solar heating contributes to the generation of valley wind circulation, producing convergence fields in mountainous areas and divergence fields in UA and SA. As a result, the amount of precipitation in the mountainous areas at around noon is greater than that in UA and SA (Fig. 3a). After 1400 LST, the urban heat island may play the dominant role in inducing a convergence zone and initiating deep, moist convection (Bornstein and Lin 2000; Baik et al. 2001; Rozoff et al. 2003; Sun et al. 2006; Sun and Shu 2007; Yin et al. 2011), resulting in increased rainfall. However, the surface heating effect in SA is weaker than that in UA, so the divergence induced by the valley wind circulation lasts until 1800 LST. At midnight, although the mountain wind should result in enhanced convergence over UA and SA, the surface cooling due to long-wave radiation is unfavorable for the ascending motion, which counters the increase in precipitation. During the early morning hours, although the mountain wind circulation is strong and the surface temperature is higher in UA than that in SA, the wind speed is reduced in UA, possibly due to its rough surface and strong mixing processes (Pielke et al. 2007; Miao et al. 2009). Consequently, a stronger convergence zone and a peak in the precipitation amount occur in the early morning in SA. Both the nocturnal and afternoon peaks of the precipitation frequency, as shown in Fig. 3b, were also attributed to the divergence associated with mountain–valley winds and the urbanization through the heat island effect by Yin et al. (2011).

7 Conclusion and discussion

By considering the conditions of the underlying surface and REOF of summer precipitation, we divided the Beijing metropolitan region into four areas: UA, SA, NMA, and SMA. Based on this division, we assessed spatial differences in diurnal variations in summer precipitation in 2004–2007, using meteorological datasets from 20 regular ground-based meteorological stations operated by the Beijing Meteorological Bureau of the China Meteorological Administration. The results show substantial differences in diurnal variations in precipitation amount in the four areas, which were verified by statistical tests. The dominant feature in NMA and UA is a single peak, at 1800 and 1900 LST, respectively. SA has two peaks, at around 0600 and 1900 LST. SMA also has two peaks, at around 0100 and 1700 LST. Moreover, the

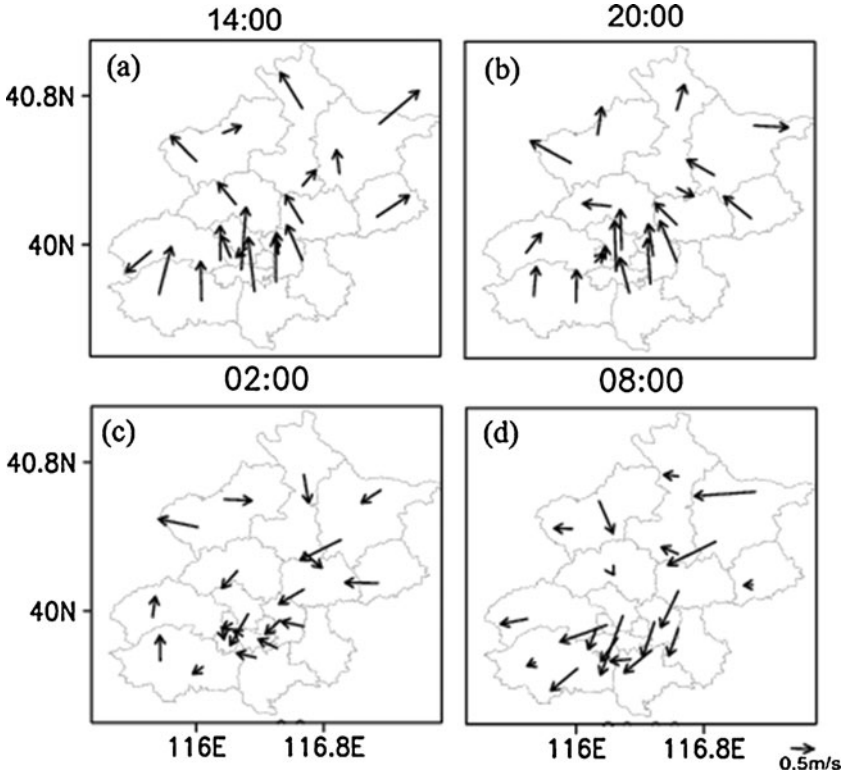

Fig. 9 Spatial distribution of surface 10-m wind vectors at **a** 1400, **b** 2000, **c** 0200, and **d** 0800 LST

mountainous areas show a minimum at 0900–1000 LST, whereas the lowest precipitation is observed in UA at about midday. Diurnal profiles of rainfall intensity resemble the profiles of rainfall amount. The temporal and spatial distributions of the normalized amount and intensity of precipitation reveal that, in the morning, SA has the most intense precipitation among the four areas, whereas in the afternoon the precipitation intensity in SMA is comparable to those in UA and SA. The temporal distribution of normalized frequency shows that from the late morning to the evening, the precipitation frequency in UA is lower than those in the other three areas, whereas the mountainous areas have the highest frequencies, followed by SA.

We explored the causes of the differences in diurnal variations in precipitation among the different areas of Beijing, revealing that the variations in precipitation are strongly related to the divergence field induced by the local circulations, which result from the different properties of the underlying surfaces and from mountain–valley circulations due to the terrain. Among others, the mountain–valley circulation induced by the mountains and the diurnal variations in thermal differences in the underlying surfaces could be important physical mechanisms, which are possibly responsible for distinct areal differences in diurnal variations in precipitation over Beijing metropolitan region.

Because of limited data availability, in this study only 4-year observational data are used. Although the diurnal cycle in precipitation in Beijing shows large interannual variations (Li et al. 2008), the present study aims to investigate differences in diurnal variations in precipitation among different areas in Beijing, and to explore the physical mechanisms that underlie these differences. We presented the features of 4-year mean diurnal variations in summer precipitation in UA, SA, NMA, and SMA over Beijing, and explained the differences in terms of the heat island effect and mountain–valley breeze. It is inevitable that year-to-year variability would exist in diurnal variations in summer precipitation. The causes of this variability may differ from those of the 4-year mean diurnal variation in precipitation examined in the present study, and other factors may be important. For example, previous studies have reported that the nocturnal or early morning rainfall peak is closely related to long-duration rainfall events and is greatly influenced by the large-scale environment, whereas the afternoon peak is dominated by short-duration rainfall events that are more closely associated with local thermal conditions (Yu et al. 2007; Chen et al. 2010; Yuan et al. 2010).

We note that some of the stations in Beijing have been changed over time in terms of site or observation protocol, which could result in abrupt changes in daily temperature and wind speed (Li and Yan 2010; Yan et al. 2010; Li et al. 2011). During the study period considered here (2004–2007), only one station (Chaoyang) was relocated, in 2007 (Yan et al. 2010); consequently, the effect of relocation on our results is likely to be insignificant. In addition, our results greatly depend on the area division because the areal mean curves are largely used. To confirm the homogeneity, we checked diurnal features of precipitation at each station in SA. The diurnal variation of the precipitation amount at each station is similar

to the area mean by exhibiting two peaks, the evening and morning peaks. At each station the evening peak is larger than the morning one except the PG station where the morning peak is a little larger, which are consistent with the peak times shown in Fig. 4. Moreover, as shown in Table 2, the precipitation diurnal variations among the four areas are significantly different. Therefore, the area division and the areal mean curves used in our present study are reasonable for investigating the diurnal variations of the precipitation in Beijing.

The present study is subjected to other limitations. First, the density of stations is relatively low in some areas, which means the data may not be entirely representative of the surrounding area. For example, UA is the area of 10 stations whereas SMA contains only 2. Second, the influences of topography on regional meteorological factors in Beijing are poorly understood, although local mountain–valley circulation is considered here. For example, the greatest precipitation amount in SA may be due to its high elevation, especially in its northern part. To overcome these deficiencies, sensitivity experiments should be performed using a numerical model, in order to further understand urban and/or topographic influences on the local climate of Beijing. Moreover, the impact of urban effects on diurnal variations in clouds and radiation warrants further research.

Acknowledgments The authors would like to thank Mr. Xiaonong Shen for his encouragement to conduct present research. We are also very grateful for the constructive comments from two anonymous reviewers. The Beijing Meteorological Bureau of the China Meteorological Administration provided the data. This study is supported by the National Science Foundation of China under Grant No. 40921003, the International S&T Cooperation Project of the Ministry of Science and Technology of China under Grant No. 2009DFA21430.

References

Andreae MO, Rosenfeld D, Artaxo P, Costa AA, Frank GP, Longo KM, Silvas-Dias MAF (2004) Smoking rain clouds over the Amazon. Science 303:1337–1342

Baik JJ, Kim YH, Chun HY (2001) Dry and moist convection forced by an urban heat island. J Appl Meteor 40:1462–1475

Balling RC, Brazel SW (1987) Recent changes in Phoenix, Arizona summertime diurnal precipitation patterns. Theor Appl Climatol 38:50–54

Bornstein RD, Lin Q (2000) Urban heat islands and summertime convective thunderstorms in Atlanta: Three case studies. Atmos Environ 34:507–516

Burian SJ, Shepherd JM (2005) Effect of urbanization on the diurnal rainfall pattern in Houston. Hydrol Process 19:1089–1103

Changnon SA (1968) The LaPorte weather anomaly—fact or fiction? Bull Am Meteor Soc 49:4–11

Chemel C, Chollet JP, Chaxel E (2007) On the suppression of the urban heat island over mountainous terrain in winter, 29th International Technical Meeting on Air Pollution Modelling and its Application, September 24, Aveiro—Portugal

Chen HM, Yu RC, Li J, Yuan WH, Zhou TJ (2010) Why nocturnal long-duration rainfall presents an eastward-delayed diurnal phase of rainfall down the Yangtze River Valley. J Climate 23:905–917

China Meteorological Administration (2003) Rules of ground surface meteorological observations. Meteorological Press, Beijing, p China

Dai AG (2001) Global precipitation and thunderstorm frequencies. Part I: seasonal and interannual variations. J Climate 14: 1112–1128

Dai AG, Deser C (1999) Diurnal and semidiurnal variations in global surface wind and divergence fields. J Geophys Res 104:109–125

Dai AG, Lin X, Hsu K-L (2007) The frequency, intensity, and diurnal cycle of precipitation in surface and satellite observations over low- and mid-latitudes. Clim Dyn 29:727–744

Diem JE, Brown DP (2003) Anthropogenic impacts on summer precipitation in central Arizona, U.S.A. Prof Geogr 55:343–355

Dou YW, Qu YG, Tao SW, Hu BK (2008) The application of quality control procedures for real-time data from automatic weather stations. Meteorol Mon (in Chinese) 34(8):77–81

Givati A, Rosenfeld D (2004) Quantifying precipitation suppression due to air pollution. J Appl Meteor 43:1038–1056

He HZ, Zhang FQ (2010) Diurnal variations of warm-season precipitation over northern China. Mon Wea Rev 138:1017–1025

Horel JD (1981) A rotated principal component analysis of the interannual variability of the northern hemisphere 500-mb height field. Mon Wea Rev 109:2080–2092

Huff FA, Changnon SA (1972) Climatological assessment of urban effects on precipitation at St. Louis. J Appl Meteor 11:823–842

Huff FA, Changnon SA (1973) Precipitation modification by major urban areas. Bull Amer Meteor Soc 54:1220–1232

Huff FA, Vogel JL (1978) Urban, topographic and diurnal effects on rainfall in the St. Louis region. J Appl Meteor 17:565–576

Jauregui E, Romales E (1996) Urban effects on convective precipitation in Mexico city. Atmos Environ 30:3383–3389

Khain A, Rosenfeld D, Pokrovsky A (2005) Aerosol impact on the dynamics and microphysics of deep convective clouds. Q J R Meteor Soc 131:2639–2663

Li Z, Yan ZW (2010) Application of multiple analysis of series for homogenization to Beijing daily temperature series (1960–2006). Adv Atmos Sci 27(4):777–787

Li J, Yu RC, Wang JJ (2008) Diurnal variations of summer precipitation in Beijing. Chinese Sci Bull 53:1933–1936

Li Z, Yan ZW, Tu K, Liu WD, Wang YC (2011) Changes in wind speed and extremes in Beijing during 1960–2008 based on homogenized observation. Adv Atmos Sci 28(2):408–420

Miao SG, Chen F, LeMone MA, Tewari M, Li QC, Wang YC (2009) An observational and modeling study of characteristics of urban heat island and boundary layer structures in Beijing. J Appl Meteor Climatol 48:484–501

Mote TL, Lacke MC, Shepherd JM (2007) Radar signatures of the urban effect on precipitation distribution: a case study for Atlanta Georgia. Geophy Res Lett 34:L20710. doi:10.1029/2007GL031903

Oke T, Musiake K (1994) Seasonal change of the diurnal cycle of precipitation over Japan and Malaysia. J Appl Meteor 33:1445–1463

Pielke RA, Adegoke J, Beltran-Przekurat A, Hiemstra CA, Lin J, Nair US, Niyogi D, Nobis TE (2007) An overview of regional land-use and land-cover impacts on rainfall. Tellus B Chem Phys Meteorol 59:587–601

Ramanathan V, Crutzen PJ, Kiehl JK, Rosenfeld D (2001) Aerosols, climate, and the hydrological cycle. Science 294:2119–2124

Ren ZH, Zhao P, Zhang Q, Zhang ZF, Cao LJ, Yang YR, Zou FL, Zhao YF, Zhao HM, Chen Z (2010) Quality control procedures for hourly precipitation data from automatic weather stations in China. Meteorol Mon (in Chinese) 36(7):123–132

Richman MB (1986) Rotation of principal components. Int J Climatol 6:293–335

Rosenfeld D (2000) Suppression of rain and snow by urban air pollution. Science 287:1793–1796

Rozoff CM, Cotton WR, Adegoke JO (2003) Simulation of St. Louis, Missouri, land use impacts on thunderstorms. J Appl Meteor 42:716–738

Sailor DJ, Lu L (2004) A top-down methodology for developing diurnal and seasonal anthropogenic heating profiles for urban areas. Atmos Environ 37:2737–2748

Shepherd JM (2006) Evidence of urban-induced precipitation variability in arid climate regimes. J Arid Environ 67:607–628

Shepherd JM, Pierce HF, Negri AJ (2002) Rainfall modification by major urban areas: observations from spaceborne rain radar on the TRMM the satellite. J Appl Meteor 41:689–701

Sun JS, Shu WJ (2007) The effects of urban heat island on winter and summer precipitation in Beijing Region. Chin J Atmos Sci (in Chinese) 31:311–320

Sun JS, Yang B (2008) Meso-β scale torrential rain affected by topography and the urban circulation. Chin J Atmos Sci (in Chinese) 32:1352–1364

Sun JS, Wang H, Wang L, Liang F, Kang YX, Jiang XY (2006) The role of urban boundary layer in local convective torrential rain happening in Beijing on 10 July 2004. Chin J Atmos Sci (in Chinese) 30:221–234

Voogt JA (2004) Urban heat islands: hotter cities. http://www.actionbioscience.org/environment/voogt.html [10-12-2006]

Wang XQ, Wang ZF, Qi YB, Guo H (2007) Preliminary inspect about the effect of urbanization on precipitation distribution in Beijing area. Climatic Environ Res (in Chinese) 12: 489–494

Wu QM, Guo H, Yang B, Sun JS (2009) Effects of topography and urban heat circulation on a meso-β torrential rain in Beijing area. Meteorol Mon (in Chinese) 35:58–64

Yan ZW, Li Z, Li QX, Jones P (2010) Effects of site chang and urbanization in the Beijing temperature series 1977–2006. Int J Climatol 30:1226–1234

Yin SQ, Li WJ, Chen DL, Jeong J-H, Guo WL (2011) Diurnal variations of summer precipitation in the Beijing area and the possible effect of topography and urbanization. Adv Atmos Sci 28(4):725–734

Yu RC, Xu YP, Zhou TJ, Li J (2007) Relation between rainfall duration and diurnal variation in the warm season precipitation over central eastern China. Geophys Res Lett 34:L13703. doi:10.1029/2007GL030315

Yuan WH, Yu RC, Chen HM, Li J, Zhang MH (2010) Subseasonal characteristics of diurnal variation in summer monsoon rainfall over central eastern China. J Climate 23:6684–6695

Zhang CL, Ji CP, Kuo Y, Fan SY, Xuan CY, Chen M (2005) Numerical simulation of topography effects on the "00.7" severe rainfall in Beijing. Prog Nat Sci 15:818–826

Zhang CL, Chen F, Miao SG, Liu QC, Xia XA, Xuan CY (2009) Impacts of urban expansion and future green planting on summer precipitation in the Beijing metropolitan area. J Geophys Res 114: D02116. doi:10.1029/2008JD010328

Zhou TJ, Yu RC, Chen HM, Dai AG, Pan Y (2008) Summer precipitation frequency, intensity, and diurnal cycle over China: a comparison of satellite data with rain gauge observations. J Climate 21 (16):3997–4010